

BOILING FLOW SIMULATION IN NEPTUNE_CFD AND FLUENT CODES

L. Vyskocil, J. Macek

Nuclear Research Institute Rez (NRI), Dept. of Thermal Hydraulic Analyses,
250 68 Rez, Czech Republic

Abstract

This paper presents simulations of the convective boiling flow performed with NEPTUNE_CFD and FLUENT codes. The DEBORA experiments carried out at CEA Grenoble were used as an experimental data set. In these experiments, freon R12 flows upwards inside a vertical pipe. Radial profiles of the flow variables are measured at the end of the heated section. Seven DEBORA cases were selected for simulation.

NEPTUNE_CFD code was used without modifications because it contains all necessary models. In FLUENT, an important part of the models has been implemented by programming in User Defined Functions. The comparison of the radial profiles of void fraction, liquid temperature, gas velocity and mean bubble diameter at the end of the heated section shows that both codes can provide reasonable results in boiling conditions.

The presented work was carried out within the 6th Framework EC NURESIM project. NEPTUNE_CFD code is implemented in the NURESIM platform.

1. INTRODUCTION

The convective subcooled boiling occurs when the heated walls are superheated while the liquid bulk is subcooled at a given operating pressure. Such a regime may occur in Pressurized Water and Boiling Water Reactors. This phenomenon can be predicted by the mechanistic boiling model of Kurul and Podowski (1990) developed at Rensselaer Polytechnic Institute. This model is implemented in NEPTUNE CFD code (Lavieville, 2005a,b). A similar boiling model was implemented in CFD code FLUENT 6 (ref. FLUENT, 2003) by programming in User Defined Functions. These two codes were used to simulate the two-phase boiling flow. The DEBORA experiments (Manon, 2000; Garnier, 2001; Bestion 2006) carried out at CEA Grenoble were used as an experimental data set.

This paper is organized as follows: chapter 2 deals with the boiling model, as implemented in FLUENT; in chapter 3, selected DEBORA experimental cases are presented; chapter 4 describes solver settings used in NEPTUNE_CFD and FLUENT calculations. The numerical results and a comparison with the experimental data are shown in Chapter 5.

2. NUCLEATE BOILING MODEL

This chapter describes the boiling model, which was implemented in FLUENT 6 code using User Defined Functions. The aim of the presented model is to simulate the onset of nucleate boiling, partitioning of wall heat flux and interfacial liquid-vapour heat, momentum and mass transfer. A very similar boiling model is included in NEPTUNE_CFD code.

The nucleate boiling model was developed for the application in the Eulerian multiphase model. Two phases are modelled: the primary phase is liquid and the secondary is vapour bubbles. The same pressure is shared by the two phases. Continuity, momentum and energy equations are solved for each phase. The realizable k- ϵ turbulence models apply to the individual phases. The distribution of the mean bubble diameter in the flow is modelled using a one-group interfacial area transport equation.

2.1 Onset of Nucleate Boiling

When the wall becomes superheated, vapour bubbles can form even when the core liquid is still subcooled. The position where the first bubbles occur at the wall is denoted as the onset of nucleate boiling. In our calculations, Hsu's criterion is used to determine this position (Lavieville, 2005b).

According to this criterion, a bubble will grow from a vapour embryo occupying a cavity in the wall if the liquid temperature at the tip of the embryo is at least equal to the saturation temperature corresponding to the bubble pressure.

2.2 Wall Heat Flux Partitioning Model

The heat flux partitioning model of Kurul and Podowski (1990) (see also Yao, Morel 2004) has the following structure:

Downstream of the onset of nucleate boiling, the wall heat flux q_{wall} is split into three parts:

$$q_{wall} = q_f + q_q + q_e \quad [W / m^2] \quad (1)$$

The first part is the single-phase heat transfer (convective heat flux):

$$q_f = A_1 \alpha_{wallfcn} (T_{wall} - T_l) \quad (2)$$

$$A_1 = 1 - A_2 \quad (3)$$

A_1 is the fraction of the wall surface influenced by liquid, fraction A_2 is influenced by vapour bubbles formed on the wall, T_l is the liquid temperature at the centre of the wall adjacent cell, $\alpha_{wallfcn}$ is the wall heat transfer coefficient calculated from the temperature wall function.

The quenching part q_q of the heat flux q_{wall} is transported by the transient conduction during the time period between the bubble departure and the next bubble formation at the same nucleation site.

$$q_q = A_2 \alpha_{quench} (T_{wall} - T_l) \quad (4)$$

α_{quench} is the quenching heat transfer coefficient (17).

The heat flux q_e is spent for evaporation of the liquid:

$$q_e = m_e H_{lat} \quad (5)$$

m_e is the evaporation mass transfer per unit wall area (15), H_{lat} is latent heat.

The model assumes that the diameter of the area influenced by a single bubble is as large as the bubble departure diameter d_w :

$$A_2 = \min\left(\frac{\pi \cdot d_w^2 \cdot n}{4}, 1\right) \quad (6)$$

n is the active nucleation site density.

Active nucleation site density is correlated to the wall superheat:

$$n = (210 \cdot (T_{wall} - T_{sat}))^{1.8} \left[\frac{1}{m^2} \right] \quad (7)$$

Bubble departure diameter d_w is calculated from Ünal correlation (Ünal, 1976):

$$d_w = 2.42 \cdot 10^{-5} p^{0.709} \frac{a}{\sqrt{b\phi}} \quad [m] \quad (8)$$

where p is pressure [Pa],

$$a = \frac{(T_w - T_{sat}) \lambda_s}{2 \rho_v H_{lat} \sqrt{\pi a_s}} \quad (9)$$

a_s is thermal diffusivity and λ_s is the thermal conductivity of the solid wall

$$b = \frac{T_{sat} - T_l}{2(1 - \rho_v / \rho_l)} \quad for \ St < 0.0065 \quad (10)$$

$$b = \frac{q_{wall}}{2(1 - \rho_v / \rho_l) \cdot 0.0065 \cdot \rho_l c_{pl} U_l} \quad for \ St \geq 0.0065 \quad (11)$$

where:

$$St = \frac{q_{wall}}{\rho_l c_{pl} U_l (T_{sat} - T_l)} \quad (\text{Stanton number}) \quad (12)$$

U_l is the liquid velocity magnitude at the wall adjacent cell

$$\phi = \max \left(1, \left(\frac{U_l}{0.61} \right)^{0.47} \right) \quad (13)$$

When $T_l > T_{sat}$, bulk boiling is initiated.

In order to calculate the evaporation rate \dot{m}_e , the bubble detachment frequency f is determined from the following equation:

$$f = \sqrt{\frac{4 \cdot g \cdot (\rho_l - \rho_v)}{3 \cdot d_w \cdot \rho_l}} \left[\frac{1}{s} \right] \quad (14)$$

The evaporation rate is the product of bubble mass, detachment frequency and the active nucleation site density:

$$\dot{m}_e = \frac{\pi \cdot d_w^3}{6} \rho_v \cdot f \cdot n \left[\frac{kg}{m^2 s} \right] \quad (15)$$

The quenching heat transfer coefficient α_{quench} depends on the waiting time between the bubble departure and the next bubble formation. This waiting time t_w is fixed to the bubble detachment period:

$$t_w = \frac{1}{f} \quad [s] \quad (16)$$

$$\alpha_{quench} = 2 \cdot \lambda_l \cdot f \cdot \sqrt{\frac{t_w}{\pi \cdot a_l}} \left[\frac{W}{m^2 K} \right] \quad (17)$$

where a_l is the thermal diffusivity of the liquid.

The presented system of equations (1) – (17) is closed, but it cannot be solved explicitly. The numerical method of bisection (Neustupa, 1995) is used to solve this system.

2.3 Interfacial Momentum Transfer

The interfacial momentum transfer can be divided into four parts: drag, virtual mass force, lift and turbulent dispersion (Lance, Lopez de Bertodano, 1994, Yao, Morel 2002, 2004).

The interfacial drag force is calculated as:

$$\vec{M}_{lv}^D = -\vec{M}_{vl}^D = 0.75 \frac{\alpha_v}{d_b} \rho_l c_D |\vec{V}_l - \vec{V}_v| (|\vec{V}_l - \vec{V}_v|) \quad (18)$$

d_b is the Sauter mean bubble diameter calculated from the interfacial area transport equation, the drag coefficient c_D is given by Ishii (1979).

The lift force is calculated as:

$$\vec{M}_{lv}^L = -\vec{M}_{vl}^L = -c_L \alpha_v \rho_l (\vec{V}_v - \vec{V}_l) \times (\nabla \times \vec{V}_l) \quad (19)$$

The lift coefficient c_L is calculated from the correlation proposed by Moraga (1999). In this correlation, the lift coefficient is calculated from the product of the bubble Reynolds number and the bubble shear Reynolds number.

The lift coefficient combines the action of the two opposing forces:

1. the classical aerodynamic lift force that results from interaction between the bubble and the liquid shear – positive influence on c_L .
2. the interaction between the bubble and vortices shed by the bubble wake – negative influence on c_L .

The virtual mass force is given by:

$$\vec{M}_{lv}^{VM} = -\vec{M}_{vl}^{VM} = c_{VM} \alpha_v \rho_l \left[\left(\frac{\partial \vec{V}_l}{\partial t} + \vec{V}_l \cdot \nabla \vec{V}_l \right) - \left(\frac{\partial \vec{V}_v}{\partial t} + \vec{V}_v \cdot \nabla \vec{V}_v \right) \right] \quad (20)$$

The virtual mass force coefficient is $c_{VM} = 0.5$.

The turbulent dispersion force is given by:

$$\vec{M}_{lv}^{TD} = -\vec{M}_{vl}^{TD} = -c_{TD} \cdot \rho_l \cdot k_l \cdot \nabla \alpha_v \quad (21)$$

The turbulent dispersion coefficient is set to $c_{TD} = 1$ (Troshko 2003, 2007). k_l is the turbulence kinetic energy of the liquid.

2.4 Interfacial Heat Transfer

Interface to liquid heat transfer (used from Yao 2002):

$$Q_{li} = h_{li} \cdot a_i (T_{sat} - T_l) \quad [W / m^3] \quad (22)$$

The heat transfer coefficient h_{li} is:

$$h_{li} = \frac{\lambda_l}{d_b} Nu \quad \left[\frac{W}{m^2 K} \right] \quad (23)$$

d_b is the Sauter mean bubble diameter.

The volumetric interfacial area a_i is given by:

$$a_i = \frac{6\alpha_v}{d_b} \quad \left[\frac{1}{m} \right] \quad (24)$$

In the case of condensation ($Ja < 0$), the Nusselt number Nu is calculated from:

$$Nu = 2 + 0.6 Re^{0.5} Pr^{0.33} \quad (25)$$

$$Re = \frac{d_b \cdot V_{rel}}{\nu_l} \quad (26)$$

Pr is the Prandtl number of the liquid, V_{rel} is the magnitude of the relative velocity between phases, ν_l is the kinematic viscosity of the liquid.

$$Ja = \frac{\rho_l \cdot c_{P,l} (T_l - T_{sat})}{\rho_v H_{lat}} \quad (\text{Jakob number}) \quad (27)$$

In the case of evaporation the Nusselt number is given by:

$$Nu = \max \left(\sqrt{\frac{4Pe}{\pi}}, \frac{12}{\pi} Ja, 2 \right) \quad (28)$$

$$Pe = \frac{d_b \cdot V_{rel}}{a_l} \quad (\text{Péclet number}) \quad (29)$$

a_l is the liquid thermal diffusivity.

Interface to vapour heat transfer:

Interface to vapour heat transfer is calculated using the “time-step return to saturation” method. It is assumed that the vapour retains the saturation temperature by rapid evaporation/condensation.

$$Q_{vi} = \frac{\alpha_v \rho_v c_{P,v}}{\delta t} (T_{sat} - T_v) \quad \left[\frac{W}{m^3} \right] \quad (30)$$

δt is the time step, $c_{P,v}$ is the isobaric heat capacity of the vapour.

The interfacial mass transfer depends directly on the interfacial heat transfer.

2.5 Interfacial Area Transport

The Sauter mean bubble diameter distribution in flow was calculated from the interfacial area concentration. One group interfacial area concentration equation with models for coalescence and break-up (Yao and Morel, 2004; Morel, Yao, Bestion, 2003, Morel 2007) is used to describe the evolution of the interfacial area concentration. A user-defined scalar equation is used to model the transport of the interfacial area in FLUENT.

3. SELECTED DEBORA TEST CASES

The boiling model was tested against DEBORA experiments carried out at the CEA (Manon, 2000; Garnier, 2001).

The DEBORA experiment is a vertical heated pipe with Freon R12 flowing upwards. At the tube inlet, R12 is a subcooled liquid. The refrigerant is heated as it flows upwards and vapour bubbles are created on the wall surface. These bubbles break away from the wall and are dispersed in the turbulent flow. The bubbles condense partly in the core region of the tube. The internal diameter of the pipe is 19.2mm. The whole pipe can be divided into three sections: the inlet adiabatic section – 1m long, the heated section – 3.5m long and the outlet adiabatic section 0.5m long. The void fraction, vapour velocity, the mean bubble diameter and interfacial area profiles were measured at the end of the heated section. Unfortunately, in this test series liquid temperature profiles were not measured.

Table 1: Selected DEBORA test cases

| Case No. | Test | pressure bar | mass flux kg/m ² /s | q _w W/m ² | T _{inlet} °C | T _{sat} °C | x _{eq} - |
|----------|--------------------|-----------------|-----------------------------------|------------------------------------|--------------------------|------------------------|----------------------|
| 1 | 29G1P30W12Te52.7_1 | 30.06 | 1006.8 | 58260 | 52.97 | 94.136 | -0.0973 |
| 2 | 29G1P30W12Te58.4_1 | 30.06 | 1007.4 | 58260 | 58.39 | 94.136 | -0.0197 |
| 3 | 29G1P30W12Te63.6_2 | 30.06 | 999.5 | 58260 | 63.43 | 94.136 | 0.0585 |
| 4 | 29G1P30W12Te68.1_1 | 30.08 | 1005 | 58260 | 67.89 | 94.136 | 0.1218 |
| 5 | 29G1P30W12Te70.4_1 | 30.07 | 1004.8 | 58260 | 70.14 | 94.136 | 0.1563 |
| 6 | 29G1P30W12Te72.9_1 | 30.07 | 1004.8 | 58260 | 72.65 | 94.136 | 0.1953 |
| 7 | 29G1P30W12Te74_1 | 30.06 | 994.9 | 58260 | 73.7 | 94.136 | 0.2173 |

q_w is the wall heat flux, x_{eq} is the outlet equilibrium vapour quality.

4. CALCULATIONS IN NEPTUNE AND FLUENT

4.1 NEPTUNE Solver Settings

Turbulence: “k-epsilon liq” model for liquid, laminar flow of vapour.

Interface momentum transfer: drag by Ishii, added mass by Zuber, no lift (lift force caused convergence troubles)

The turbulent dispersion force is based on the void fraction gradient – see eq. (21), the turbulent dispersion coefficient was set to c_{TD}=2.5. This value was taken from ref. Yao (2002), note that this is a different value than that used in FLUENT calculations (c_{DT} = 1). If c_{DT} = 2.5 is used in FLUENT it spoils the results – it overestimates mixing. On the other hand, if c_{DT} = 1 is used in NEPTUNE, it provides insufficient mixing.

Wall-fluid heat transfer: Grenoble models (no superheating of the vapour, same models as in chapter 2.2)

Interface heat transfer: Grenoble models for liquid and vapour (same models as in chapter 2.4)

Physical properties of fluid R12: CATHARE tables.

The *particle diameter* was calculated from the interfacial area concentration, Yao (2002) model was used for coalescence and fragmentation.

NEPTUNE version: 1.0.5

4.2 FLUENT Solver Settings

Models used in FLUENT calculations were described in chapter 2.

Solver: segregated, 1st order implicit unsteady formulation, Eulerian multiphase model.

Turbulence: realizable k-epsilon model solved per phase

Discretisation: second-order upwind for convection terms in all equations except for the user defined scalar, user-defined scalar equation: first order upwind (used for calculating the interfacial area)

Physical properties of fluid R12: piecewise-linear profiles based on NIST Chemistry WebBook.

FLUENT version 6.1.22

4.3 Main Differences Between NEPTUNE and FLUENT Calculations

- turbulence models
- lift force
- turbulent dispersion coefficient
- physical properties of fluid R12

4.4 Computational Grid

The case is axisymmetric, a 10° wedge confined with symmetry cutting planes is used to model the pipe.

Grid Resolution:

radius: 14 intervals

axial direction: 200 intervals - inlet section (1m long)

700 intervals - heated section (3.5m long)

100 intervals - outlet section (0.5m long)

Wedge cells in the centre of the pipe are included in the grid for FLUENT (Fig. 1), while in NEPTUNE they had to be omitted and replaced with a small symmetry cutting plane (because of convergence troubles).

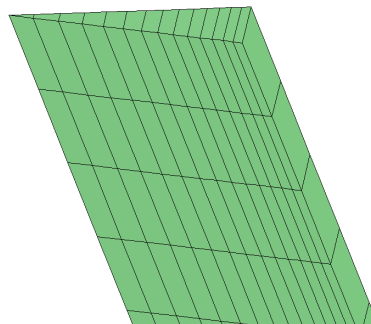


Fig. 1 Computational Grid

Note: A grid independence test was performed – see chapter 5.2.

5. RESULTS

The following figures show the radial profiles at the end of the heated section.

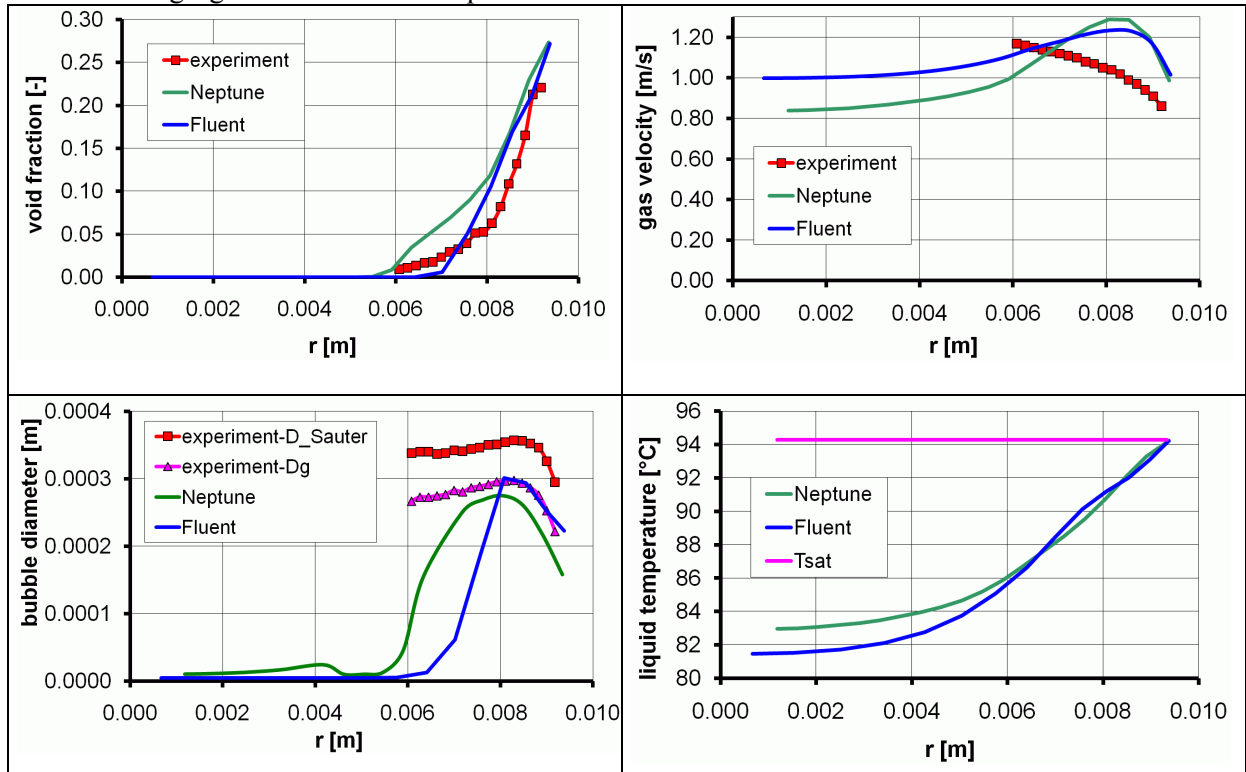


Fig. 2 Results: Case 1 – $T_{in} = 52.97^{\circ}\text{C}$, $x_{eq} = -0.0973$

Note: Diameter D_g corresponds to an equivalent two-phase flow (keeping the bubble centre density and the interfacial area density) where all the bubbles are assumed to have the same diameter, see Manon (2000).

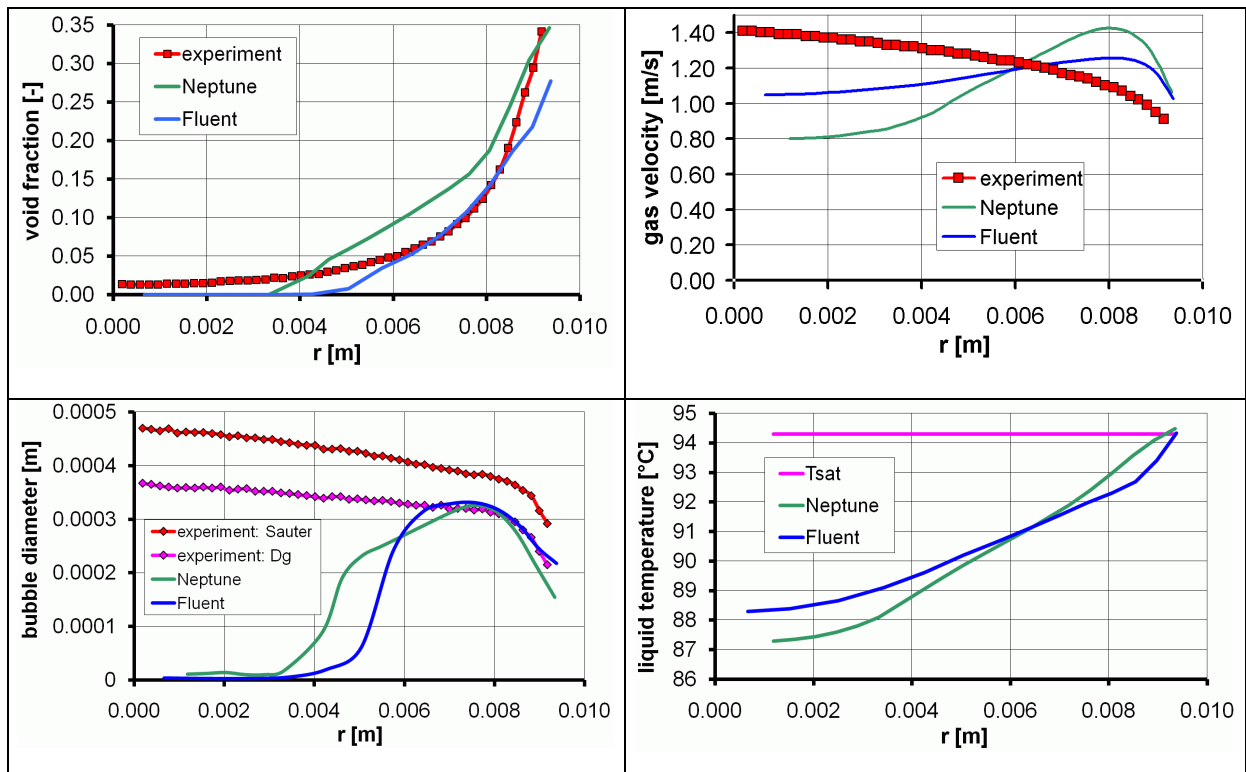


Fig. 3 Results: Case 2 – $T_{in} = 58.39^{\circ}\text{C}$, $x_{eq} = -0.0197$

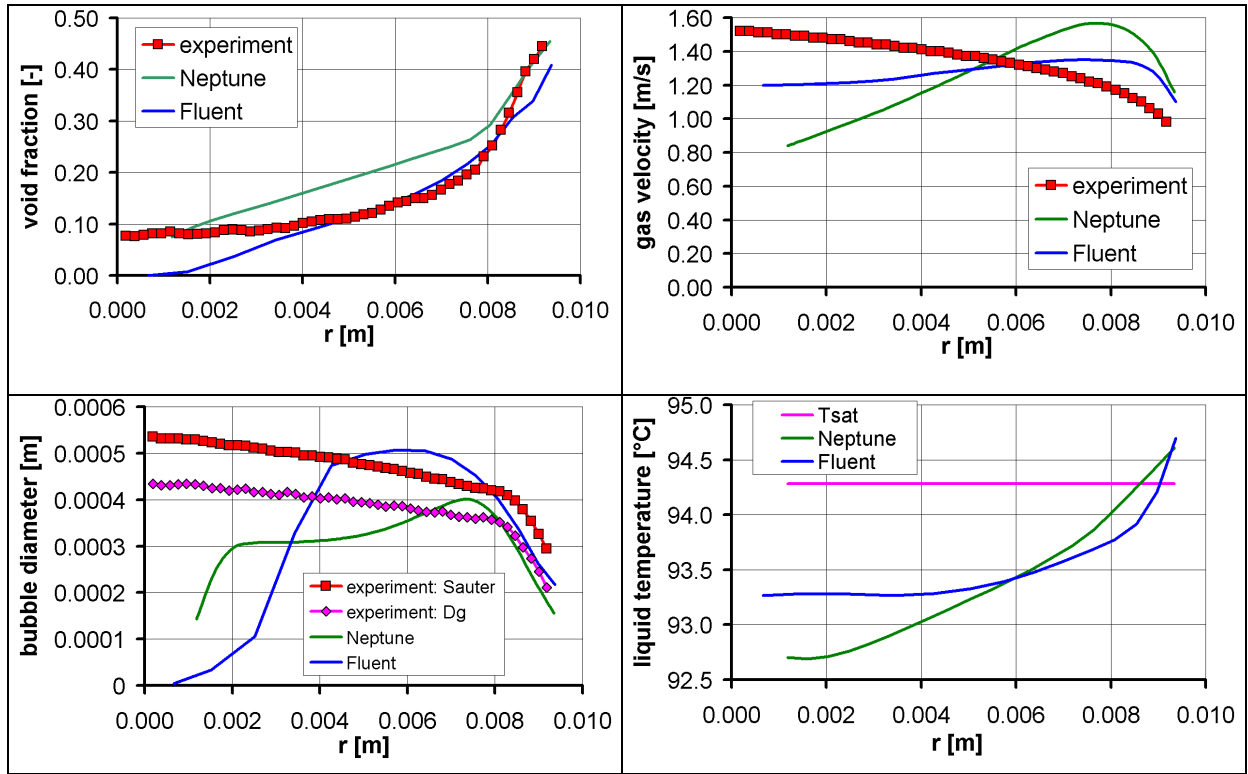


Fig. 4 Results: Case 3 – $T_{in} = 63.43^{\circ}\text{C}$, $x_{eq} = 0.0585$

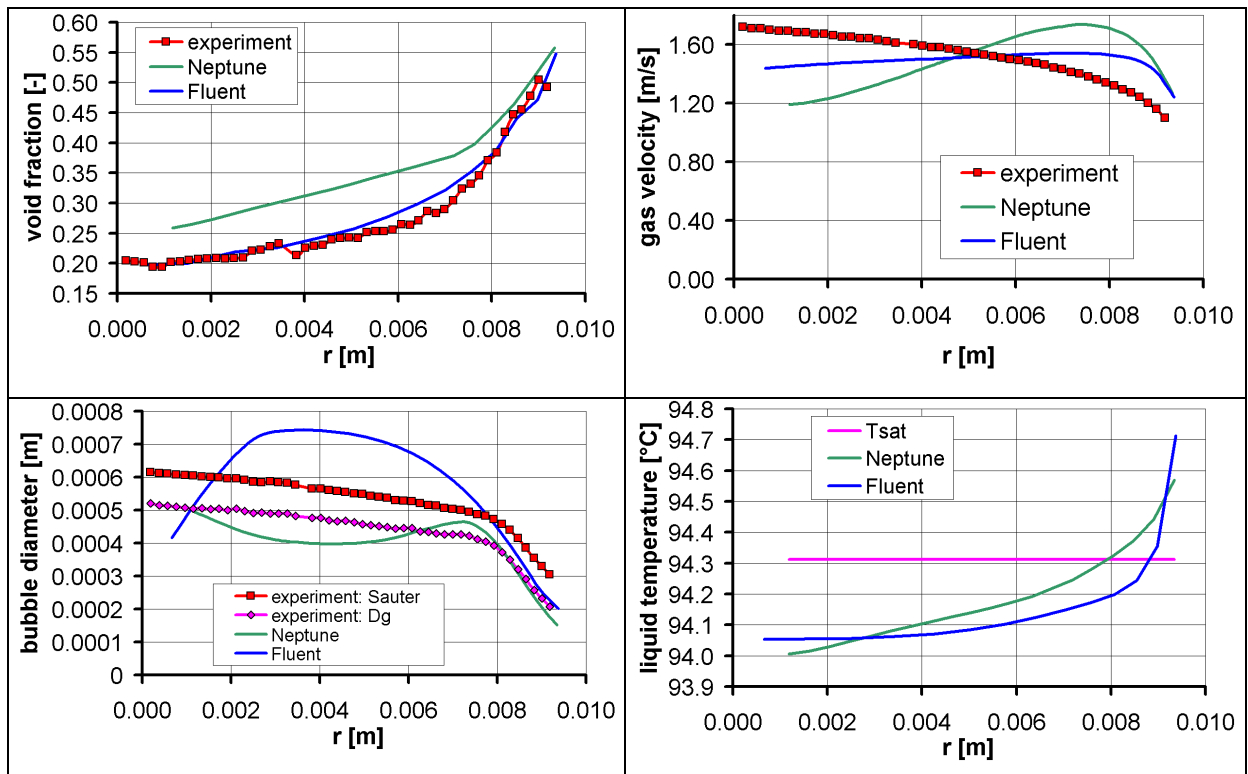


Fig. 5 Results: Case 4 – $T_{in} = 67.89^{\circ}\text{C}$, $x_{eq} = 0.1218$

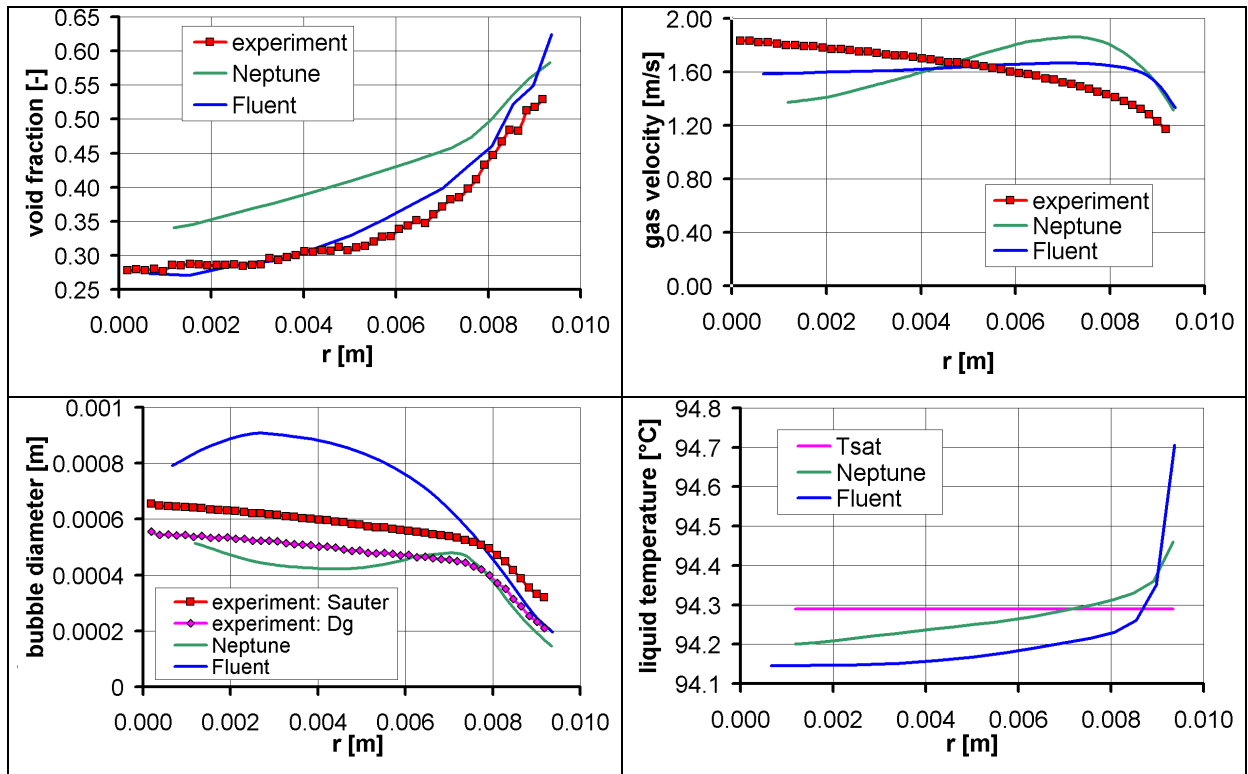


Fig. 6 Results: Case 5 – $T_{in} = 70.14^\circ\text{C}$, $x_{eq} = 0.1563$

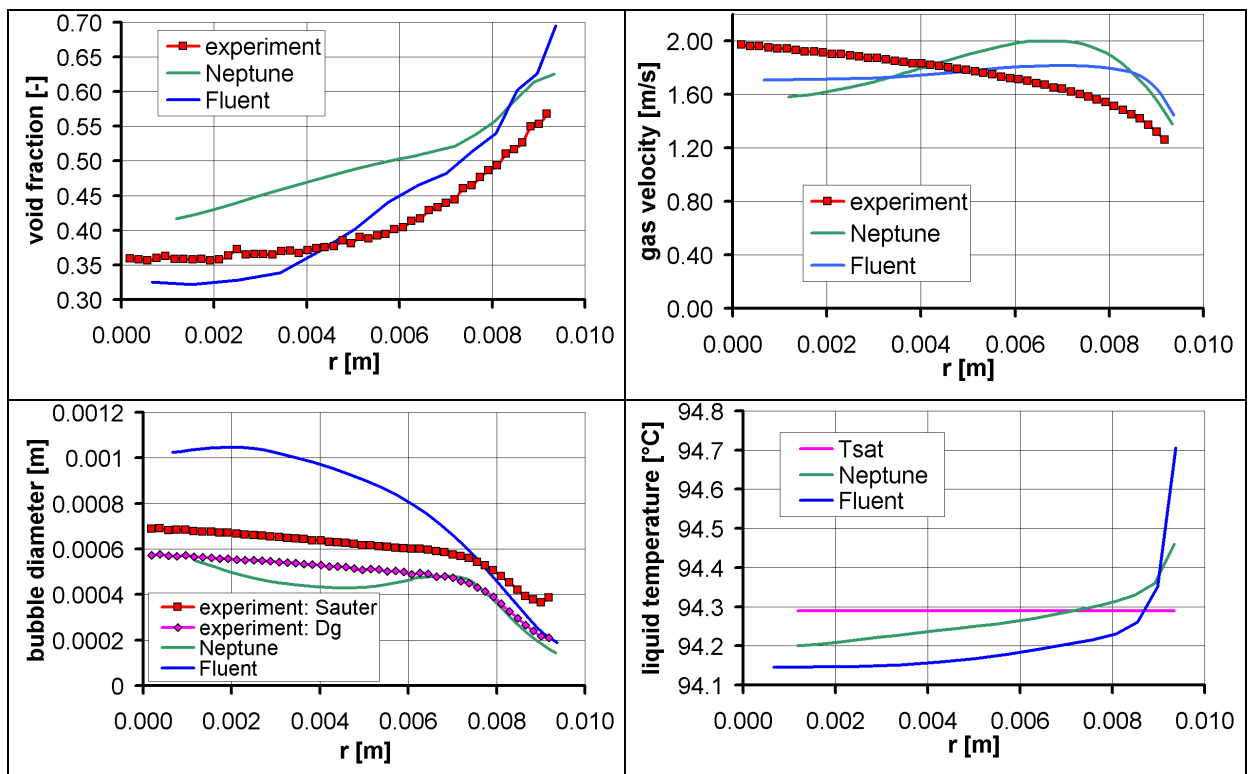


Fig. 7 Results: Case 6 – $T_{in} = 72.65^\circ\text{C}$, $x_{eq} = 0.1953$

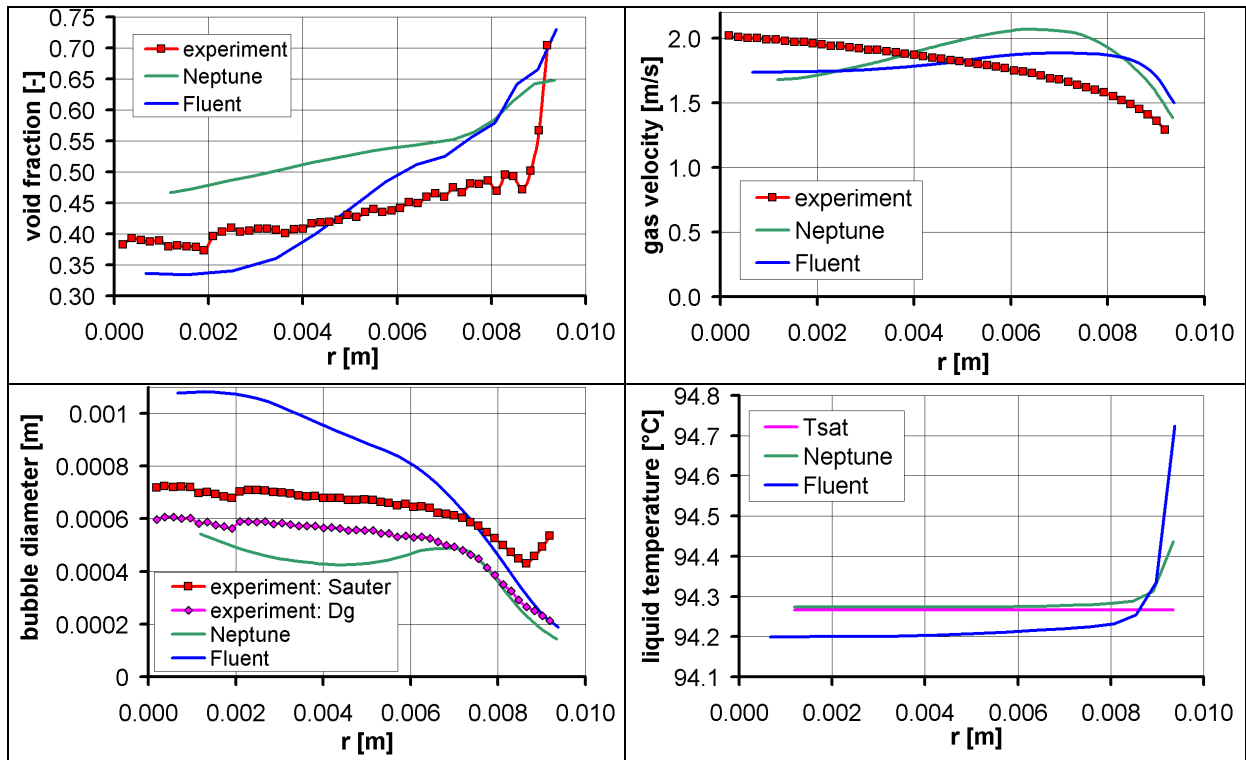


Fig. 8 Results: Case 7 – $T_{in} = 73.7^{\circ}\text{C}$, $x_{eq} = 0.2173$ (close to DNB)

5.1 Problem – overestimated bubble diameter in FLUENT calculations

The turbulence model in FLUENT provides a lower epsilon in the core of the flow than NEPTUNE. The coalescence and break-up terms in Yao's interfacial area transport model depend on epsilon. A lower epsilon causes exaggerated coalescence and decrease of break-up in the duct centre, which in turn leads to overestimated bubble diameter. This problem can be seen in Fig. 5 - Fig. 8.

Attempt to solve this problem in FLUENT:

The coalescence and break-up terms use the function $\max(\text{epsilon}, 0.13\text{m}^2/\text{s}^3)$ instead of epsilon.

The following figures compare the results obtained with this modification and without this modification.

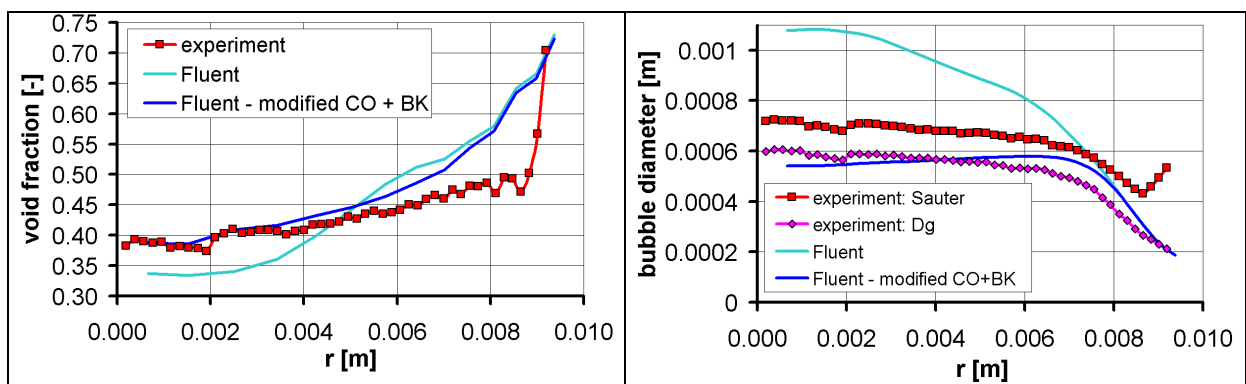


Fig. 9 Results - Case 7: modification of the coalescence and break-up model in FLUENT can provide more realistic values of bubble diameter in the duct centre

The influence of this modification on the liquid temperature and vapour velocity profile is not so marked.

5.2 Grid Independence Test

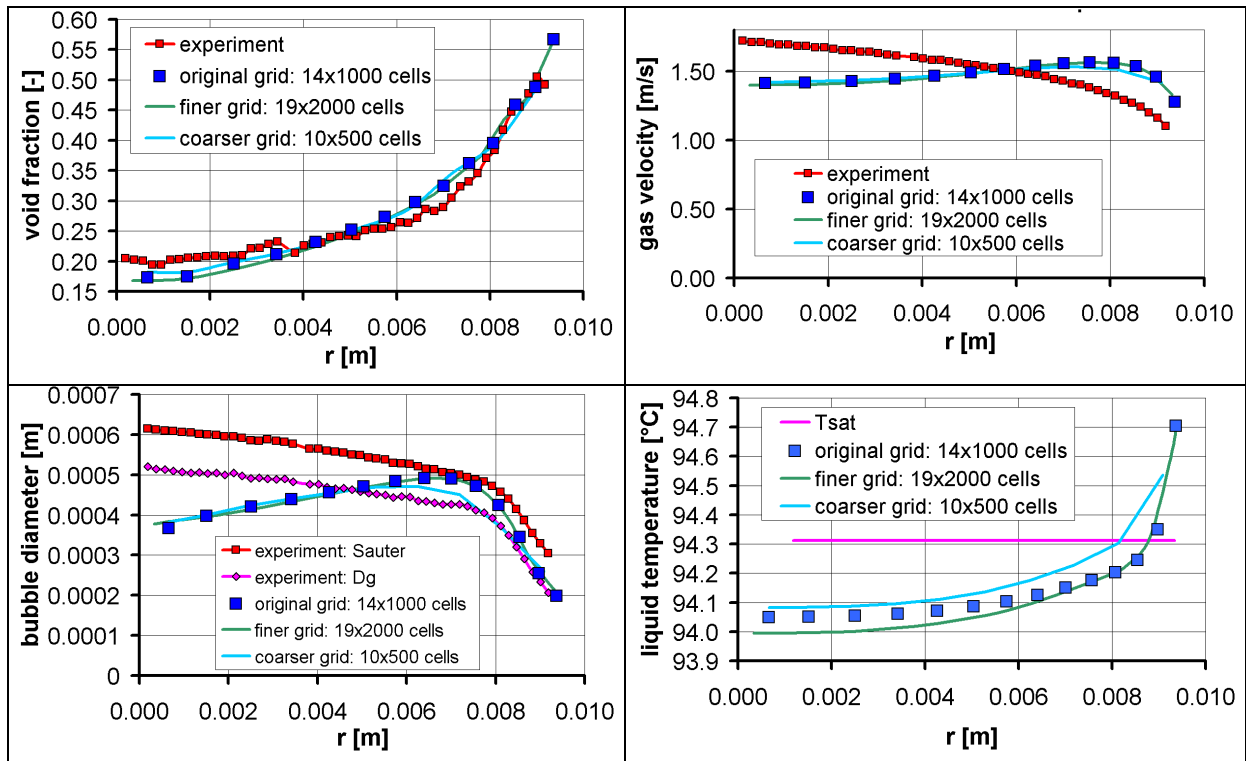


Fig. 10 Case 4 – FLUENT: grid independence test

From the above figure it can be seen that the original grid is fine enough and grid refinement does not improve the results of FLUENT calculations. Grid independence was also tested in NEPTUNE with the same conclusion.

Note: The modified coalescence and break-up model from the previous page was used in these calculations.

6. CONCLUSIONS

The capability of CFD codes to simulate convective boiling flow in a vertical tube has been demonstrated. Seven DEBORA tests have been simulated with NEPTUNE_CFD and FLUENT codes. In these cases, the equilibrium outlet vapour quality ranges from -0.0973 to $+0.2173$ (close to DNB). The interfacial area transport was modelled in both codes. The main differences in the modelling used with the two codes were as follows: turbulence models, the turbulent dispersion coefficient, lift force and the physical properties of fluid R12. An important part of the models has been implemented in FLUENT by programming in User Defined Functions.

FLUENT and NEPTUNE CFD codes provided comparable results. Reasonable agreement with experimental data was obtained.

In tests with a higher inlet temperature NEPTUNE overestimates the void fraction in the core of the flow while Fluent overestimates the void fraction near the wall.

NEPTUNE slightly underestimates the mean bubble diameter. If Yao's interfacial area model is used in FLUENT, it causes overestimation of the bubble diameter in the duct centre, this problem could be solved by modifying the epsilon values used by Yao's model.

In the last case close to DNB, a sudden rise of a void fraction close to the wall was observed in the experiment. While the maximum value of the void fraction at the wall was captured well by the two codes, the shape of the void fraction peak near the wall was not reproduced in either of the codes. In the near-wall region, the calculated void fraction profiles are more mixed than the experimental profile.

It is interesting that to obtain the best results, different turbulent dispersion coefficients had to be used in the two codes.

REFERENCES

- Bestion, D., Caraghiaur, D., Anglart, H., Péturaud, P., Krepper, E., Prasser, H M., Lucas, D., Andreani M., Smith B., Mazzini D., Moretti F., Macek J.: “Deliverable D2.2.1: Review of the Existing Data Basis for the Validation of Models for CHF”, *NURESIM SP2 Deliverable* (2006).
- Garnier J., Manon E., Cubizolles G.: “Local measurement on flow boiling of Refrigerant 12 in a vertical tube”, *Multiphase Science and Technology*, Vol.13, pp.1-58 (2001).
- Ishii, M., Zuber, N.: “Drag coefficient and relative velocity in bubbly, droplet or particulate flows”, *AIChE Journal Vol.25, No.5*, pp. 843-855 (1979)
- Kurul, N., Podowski, M.Z.: “Multidimensional Effects in Forced Convection Subcooled Boiling”, *Proceedings of the 9th International Heat Transfer Conference*, Jerusalem, Israel, 21-26 August (1990)
- Lance M., Lopez de Bertodano M.: “Phase distribution phenomena and wall effects in bubbly two-phase flows”, *Multiphase Science and Technology* 8, pp. 69-123 (1994)
- Lavieville, J., Quemerais, E., Boucker, M., Maas, L.: “NEPTUNE CFD V1.0 User Guide (Draft)”, EDF (2005a).
- Lavieville, J., Quemerais, E., Mimouni, S., Boucker, M., Mechitoua, N.: “NEPTUNE CFD V1.0 Theory Manual”, EDF (2005b).
- Manon, E.: “Contribution a l'analyse et a la modélisation locale des écoulements bouillants sous-saturés dans les conditions des réacteurs a eau sous pression.” These de Doctorat. Ecole Centrale Paris (2000).
- Moraga, F.J., Bonetto, F.J., Lahey, R.T.: “Lateral forces on spheres in turbulent uniform shear flow”, *Int. J. Multiphase Flow* 25, pp.1321-1372, (1999).
- Morel, C., Yao, W., Bestion, D.: “Three Dimensional Modeling of Boiling Flow for the NEPTUNE Code”, *NURETH-10*, Seoul, Korea, October 5-9 (2003).
- Morel C.: “Deliverable D2.2.1.3: Validation of NURESIM CFD against DEBORA tests close to CHF conditions”, *NURESIM SP2 Deliverable* (2007).
- Neustupa, J.: “Matematika 1”, Czech Technical University In Prague (1995).
- Troshko A.: “Implementation and Testing of Subcooled Boiling Model”, Fluent Technical Notes, TN228, Fluent.Inc (2003).
- Troshko A., Schowalter D., Guetari Ch.: “CFD Validation Benchmark of Subcooled Nucleate Boiling Under Near Saturation Conditions”, *NURETH-12*, Pittsburgh, PA, USA, Sept 30-Oct 4 (2007).
- Ünal, H.C.: “Maximum bubble diameter, maximum bubble growth time and bubble growth rate during subcooled nucleate flow boiling of water up to 17.7MW/m^2 ”, *Int. J. Heat Mass Transfer* 19, pp.643-649, (1976)
- Yao, W., Morel, C.: “Prediction of Parameters Distribution of Upward Boiling Two-Phase Flow with Two-Fluid Models”, *ICONE10-22463*, April 14-18 (2002).

Yao W., Morel C.: “Volumetric interfacial area prediction in upward bubbly two-phase flow”, *Int. J. Heat and Mass Transfer* 47, pp.307-328 (2004).

“FLUENT 6.1 User’s Guide”, Fluent Inc., Lebanon NH, USA (2003).

“NIST Chemistry WebBook, Thermophysical Properties of Dichlorodifluoromethane (R12)”, *National Institute of Standards and Technology*, <http://webbook.nist.gov/>